Molecular Motion in the Two Amorphous Phases of Triphenyl Phosphite

S. Dvinskikh,[†] G. Benini,[‡] J. Senker,[‡] M. Vogel,[‡] J. Wiedersich,[‡] A. Kudlik,[‡] and E. Rössler*[,‡]

Institute of Physics, St. Petersburg State University, Ulyanovskaya 1, 198904 St. Petersburg, Russia, and Physikalisches Institut, Universität Bayreuth, Universitätsstrasse 30, D-95440 Bayreuth, Germany

Received: August 19, 1998; In Final Form: December 2, 1998

Molecular reorientation in the two amorphous phases of triphenyl phosphite, namely the supercooled liquid (phase aI) and the newly discovered second amorphous phase (phase aII), was investigated by dielectric relaxation and by two-dimensional (2D) nuclear magnetic resonance spectroscopy (NMR) in the time and frequency domain. Whereas phase aI exhibits the relaxational features typical of supercooled liquids, the molecular motion in phase aII is characterized by an extremely broad dielectric loss and by a pronounced nonexponential reorientational correlation function. Using a Gaussian distribution of correlation times, both dielectric and NMR data reveal consistently correlation times on the order of seconds. The quantitative analysis of the 2D spectra favors the interpretation that molecular motion in phase aII leads to an isotropic distribution of molecular orientation on the surface of a sphere. In addition, we find a secondary relaxation process that shows basically the same features in both phases. We conclude that the newly discovered phase is a second liquid phase with a very unusual reorientational correlation function. However, a nematic liquid crystal cannot completely be ruled out.

Introduction

In 1996 Kivelson and co-workers[1,2] reported the discovery of a new apparently amorphous phase of the glass former triphenyl phosphite (TPP). This phase is formed from the supercooled, viscous liquid (phase aI) via a first-order phase transition and was called the glacial phase (phase aII). Its physical properties are well distinguished from that of the glass obtained by cooling the liquid with a rate faster than 10 K/min.[1−6] For example, density, sound velocity, and spin−lattice relaxation times differ. The new phase is believed to be amorphous because X-ray diffraction does not show any Bragg peaks. Its structure factor $S(q)$ resembles that of the conventionally formed glass except that the main peak of $S(q)$ is slightly shifted to higher q values.[2,7]

While the melting point T_m of TPP is 295 K, the glass transition temperature T_g has been identified to be 205 K.[3,4] The transformation from phase aI to phase aII can easily be observed in the temperature range 215−230 K. Here the phase transformation occurs on the time scale of minutes to hours. At higher temperatures phase aII quickly transforms into the crystalline state. Thus, phase aII is metastable with respect to the crystal. The transformation from phase aI to aII is accompanied by the appearance of turbidity, which at the end of the transformation disappears almost completely.[2,4] The lack of complete clearing particularly at high temperatures may be due to the slow onset of crystallization. In our previous study[4] we demonstrated by investigating the dielectric loss that the new phase exhibits pronounced molecular motion. As compared to the supercooled liquid, a very broad loss curve unusual for neat molecular systems was observed. These results correspond to those reported by Johari and Ferrari.[5] Also, the comparatively short spin−lattice relaxation provides indications that reorientational motion is present.[1,2,4] Correlation times obtained for phase aII are much longer compared with those of the supercooled liquid, but their temperature dependences are similar. Attempting to fit the temperature dependence of the correlation times in phase aII with an Arrhenius law leads to an apparent activation energy $E_A = 250$ kJ/mol and an exponential prefactor $\tau_0 = 10^{-58}$ s. This unphysically low prefactor can be taken as a hint that no single particle motion but rather some collective motion is involved, as in the case of supercooled liquids, where the main relaxation process, namely the α-process, is believed to be of cooperative nature.

The phenomenon of two amorphous solid-state phases for a given system has gained increasing interest in the last years and the term polyamorphism[1,8] has been applied in analogy to the term polymorphism in the case of crystalline systems. The most prominent example is amorphous H_2O, where a transition from a high-density to a low-density amorphous state is found.[9] Also, other systems such as Y_2O_3/Al_2O_3 or Si show this phenomenon.[10] Mostly, the nature of the second amorphous phase is unclear, yet. Here, of course, we have to admit that also the structure of conventional glasses is not completely understood. Several speculations are found in the literature.[1,2] From simulation studies it was concluded that structural changes occur.[10] For example, an abrupt drop of the density was found, simulating a silicon melt, and was associated with a small decrease in the coordination number. In the case of SiO_2 a change from a 4-fold to a 6-fold coordination was observed by applying pressure within a molecular dynamics study.[8] All these examples refer to systems with more or less pronounced chemical network structures.

In contrast to this, TPP is a molecular system and therefore has to be distinguished. Kivelson and co-workers interpreted the second amorphous phase of TPP as a defect ordered crystal.[1,2] Domains of nanocrystallites were discussed in a Raman scattering study by Hédoux et al.[6] Johari and Ferrari considered the possibility of an orientationally disordered crystal or a liquid crystal.[5] Comparing the temperature dependence of

[†] St. Petersburg State University.
[‡] Universität Bayreuth.

10.1021/jp983411z CCC: $18.00
Published on Web 02/20/1999

the motional correlation times we previously discussed the possibility of the presence of two kinds of viscous liquids, namely fragile and strong glass formers.[4] This idea was already introduced by Angell et al. and Poole et al.[10,11]

In this contribution we want to focus on characterizing the nature of the molecular motion in both the supercooled liquid and the newly discovered phase of TPP in more detail. In particular we are interested in unraveling the type of molecular reorientation in phase aII. The transformation from phase aI to aII might be a first-order liquid−liquid transition or it might be a transition to a completely new solid-state structure, for example, a defect ordered crystal. The extent of angular restrictions imposed on the molecular reorientation is expected to be significantly larger in the solid-state structure. Therefore, clarifying the type of motion will allow important conclusions concerning the nature of the new phase. Since both phases aI and aII exhibit slow dynamics, we applied two-dimensional (2D) NMR in the time as well as in the frequency domain. 2D NMR provides direct access to the corresponding correlation function, giving the chance to reveal details of molecular reorientation. We applied ^{31}P NMR, which is well suited because a TPP molecule contains a single phosphorus atom in its center. As a consequence, dipolar couplings can be ignored in the first approximation and the chemical shift anisotropy dominates the ^{31}P NMR spectra. Together with new data from dielectric relaxation measurements, we will present a combined analysis of the main relaxation process in phase aII. Also, we will demonstrate that both amorphous phases exhibit a secondary relaxation process that essentially is not changed by the phase transition. In addition, we report data on the time scale of the transformation from the supercooled liquid to the new phase obtained by differential scanning calorimetry. All our results are consistent with the interpretation that the second amorphous phase of TPP is a liquid with very anomalous molecular reorientation on an extremely long time scale.

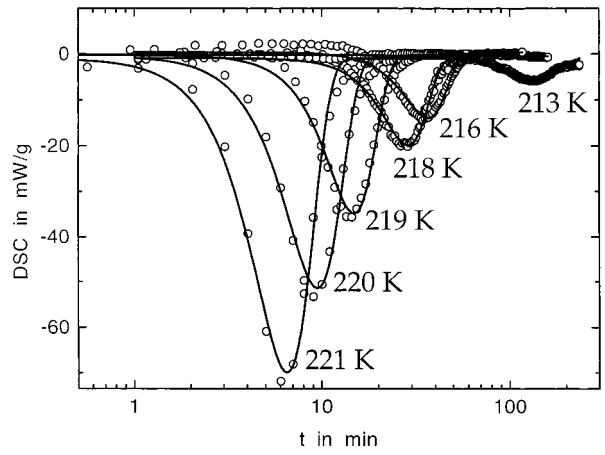

Figure 1. DSC curves at constant temperature. The heat release during the transition from the supercooled liquid to the second amorphous phase is monitored. Solid line: fit by eq 1.

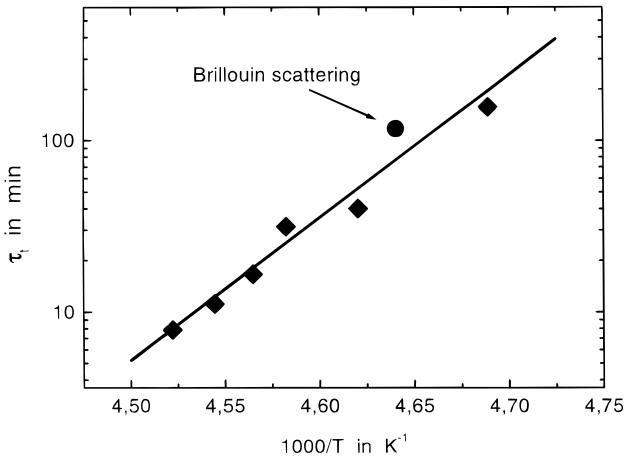

Figure 2. Transformation times τ_t as revealed by the Avrami fit of the data in Figure 1. Solid line: Arrhenius fit with an activation energy $E = 130$ kJ/mol.

Experimental Section

Triphenyl phosphite (TPP) was purchased from Acros (99% purity) and from Merck (97% purity) and was used without further purification. For the NMR measurements the sample (Acros) was degassed by the standard freeze-and-pump technique in a 5 mm ampule and sealed off under vacuum. To transform the supercooled liquid into the second amorphous phase (phase aII), we first cooled the liquid to a temperature slightly above the glass transition point ($T_g = 205$ K) with a cooling rate of about 10 K/min to avoid crystallization. Then the sample was heated to 218 K and was kept at this temperature. Within 2 h the transformation process was completed, which can easily be monitored by continuously measuring the spin−lattice relaxation time[4] (cf. Figure 10).

We also studied the isothermal phase transformation by differential scanning calorimetry (DSC). As reported,[3,4] the transition from the supercooled liquid to phase aII is characterized by a large change of enthalpy. The time scale of the transition can be estimated by isothermal DSC measurements, where the heat release is monitored during the transition. Typical curves are shown in Figure 1. To get the time constant of the transition at a given temperature, we applied the Avrami equation,[12] in particular, its time derivative is applied for the data in Figure 1. Explicitly,

$$\frac{dN(t)}{dt} = N_o n \tau_t^{-n} t^{(n-1)} e^{-(t/\tau_t)^n} \quad (1)$$

$N(t)$ is the number of molecules transformed to phase aII, and N_o is the total number of molecules; τ_t is the characteristic time constant, and n is the Avrami exponent. The Avrami equation fairly reproduces the data, although deviations occur at the wings of the DSC curves. We find the exponent n to be in the range 3−4. The corresponding time constant τ_t is plotted as a function of reciprocal temperature in Figure 2. Clearly, an Arrhenius behavior with activation energy $E = 130$ kJ/mol was found. The time constants well agree with the corresponding time constants obtained from dielectric, Brillouin, and Raman scattering[4,6] experiments.

We note that the Acros and Merck samples did not show any significant difference in the phase transformation properties. Moreover, adding benzene to a TPP sample did not change the appearance of the different phases. Only at concentrations higher than 5 wt % is the transformation slightly shifted to lower temperatures, as revealed by the DSC runs. Therefore, it appears that the formation of the second amorphous phase is not strongly dependent on the degree of purity.

The ^{31}P NMR (spin $I = 1/2$) measurements were carried out on a Bruker DSX 400 spectrometer operating at a resonance frequency of 162 MHz, which corresponds to an external magnetic field $B_0 = 9.3$ T. The length of the 90° pulse was adjusted to 2.4 μs. The spectrometer dead time did not exceed 6 μs. A gas flow-temperature controller (Bruker VT-2000) with an additional thermocouple was applied for sample temperature

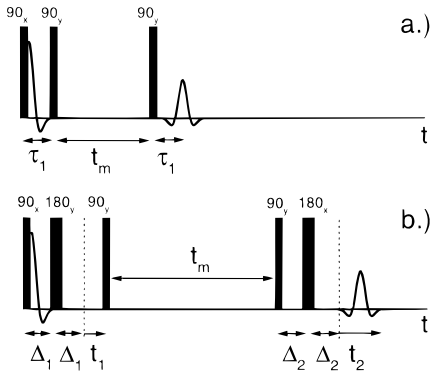

Figure 3. (a) Three pulse sequence generating the stimulated echo after the third pulse. An extended 4-fold phase cycling was used with the following phases of the three 90° pulses and the receiver phase: (1) $+x, +y, +y, -y$; (2) $+x, -y, +y, +y$; (3) $-x, +y, +y, +y$; (4) $-x, -y, +y, -y$. (b) Five pulse sequence applied for recording the 2D exchange spectra; second and fifth pulses are 180° pulses to generate a Hahn echo. We used an 8-fold phase cycling, which coincides with that of ref 13 for the cosine and sine part.

adjustment. The sample temperature was set with an accuracy of 1 K and stabilized to ±0.1 K.

The one-dimensional (1D) solid state ^{31}P spectra were recorded by applying a Hahn echo pulse sequence with a 16-fold phase cycling, and the spin−lattice relaxation time (T_1) was measured with a saturation-recovery sequence. To probe directly the reorientational correlation function $f_2(t)$ (cf. eq 3), we applied the stimulated echo pulse sequence displayed in Figure 3a. The stimulated echo amplitude was monitored by varying the mixing time t_m. Spin−spin (T_2) and spin−lattice relaxation times (T_1), which are in the range of hundreds of microseconds and tens of seconds, respectively, provide the limits of the time window of the stimulated echo experiment. In the present study the short time limit was extended to the microsecond range by applying a 4-field phase cycling,[13] which compensates contributions from single quantum coherences (cf. Figure 3a). The intensity of the zero-quantum and multiquantum coherences was assumed to be negligible because of nearly isolated phosphorus nuclei in TPP.[14] As a consequence, we increased the time window by almost two decades as compared to the results presented in ref 15. The two-dimensional (2D) exchange NMR spectra were recorded by applying a five-pulse extension of the standard exchange experiment, allowing us to overcome receiver dead time problems.[13] The fixed delays Δ_1 and Δ_2 were set to 20 μs (cf. Figure 3b). Two data sets corresponding to real (cosine) and imaginary (sine) parts were recorded in separate experiments and the States algorithm of the 2D Fourier transform[16] was used to obtain the pure absorption-mode 2D spectra. A sweep width of 512 kHz with 512 data points in both frequency directions was employed, and an effective broadening of 4 kHz was used. An 8-fold phase cycling to remove artifacts from refocusing pulses and T_1 effects was applied.[13,16] Sixteen scans for both the cosine and sine part were accumulated. No proton decoupling was applied in the present study because the chemical shift tensor is well resolved already without decoupling.

For the dielectric measurements the Merck sample was used. Two microscope glass plates were partially covered with silver, glued together at a distance of 50 μm, and filled with the sample. Dielectric data were recorded in the frequency range 10^{-2} Hz $< \nu < 10^5$ Hz with a Schlumberger SI 1260 frequency response analyzer in connection with the current to voltage converter BDC from Novocontrol. The stability of the temperature during a frequency sweep was ±0.2 K.

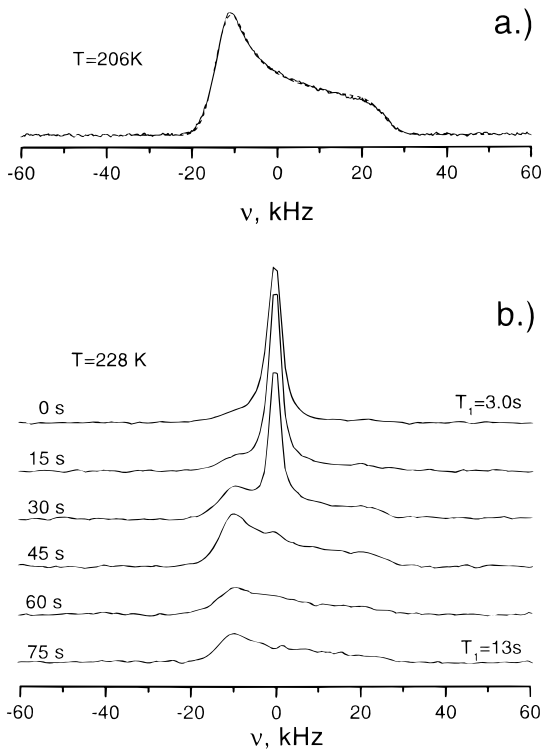

Figure 4. (a) ^{31}P NMR spectrum of supercooled TPP at 206 K (solid line) compared with the numerically calculated powder spectrum (dashed line): anisotropy parameter $\Delta\sigma\nu_0 = 38.3$ kHz ($\Delta\sigma = 236$ ppm), asymmetry parameter $\eta = 0$. For the experimental data a Lorentzian broadening of 300 Hz and for the simulation a Gaussian broadening of 4 kHz were used to describe additional spin couplings. (b) ^{31}P NMR spectra recorded during transition from the supercooled liquid to the second amorphous phase aII at $T = 228$ K. "Single shot" spectra were measured each 15 s; time and T_1 for the first spectrum (aI phase) and for the last one (aII phase) are indicated.

Results

As mentioned before and already reported in refs 1, 2, and 4, the ^{31}P spin−lattice relaxation time in the second amorphous phase (aII) is well distinguished from the one in both the supercooled liquid and the crystal. The short T_1 values at high temperatures ($T < 230$ K) demonstrate the presence of molecular motion in phase aII. However, for a given temperature, T_1 is somewhat longer than that in the supercooled liquid. Since T_1 increases with decreasing temperature, we expect that the molecular reorientation is in the slow motion regime, i.e., $\omega_0\tau \geq 1$ where ω_0 is the Larmor frequency. In addition to measuring the 1D spectra and the spin−lattice relaxation time, we applied 2D NMR in order to investigate the slow molecular motion. For comparison also the dynamics in the supercooled liquid was studied.

1. NMR Spectra. The ^{31}P NMR solid state spectra (1D spectrum) of TPP in phase aII and in the supercooled liquid (phase aI) are determined by an axially symmetric chemical shift tensor with an anisotropy parameter $\Delta\sigma\nu_o = 38.3(8)$ kHz ($\Delta\sigma = 236.6$ ppm), which characterizes the width of the spectrum (cf. Figure 4a).[17] For the supercooled liquid the fast motional limit is reached above 228 K; accordingly, the NMR spectrum is represented by a narrow single Lorentzian line (Figure 4b, top). At this temperature the transition to phase aII occurs on a time scale of minutes and can directly be observed as the ^{31}P NMR spectrum transforms from a narrow liquidlike line to a broad chemical shift tensor spectrum (Figure 4b, bottom). The estimated relaxation time value T_1(aII) ≅ 13 s at the end of transformation is considerably longer than that at

the beginning of the transformation in the liquid phase aI T_1(aI) $\cong$ 3 s. The sample stays in this phase for a few minutes and then crystallizes, leading to an even longer relaxation time T_1(crystal) $\cong$ 150 s. The NMR spectrum in the crystal is essentially indistinguishable from the one in phase aII and also from the one in the conventional glass at $T < 205$ K. This is not surprising because the chemical shift tensor is a molecular property. From these findings it is obvious that molecular motion in phase aII is slow with respect to the time scale of the 1D spectra at temperatures $T \leq 228$ K. Hence, we expect molecular motion occurring on times longer than approximately 100 μs. To resolve such slow reorientational processes, we have to recourse to two-dimensional (2D) NMR. Whereas the analysis of 2D spectra reveals information on the reorientational angles involved in the molecular motion, the same pulse sequences can be applied to study directly reorientational correlation functions. Both types of measurements will be discussed here. We start with the time domain experiments.

2. Analysis of the Stimulated Echo Decays. By applying a stimulated echo three pulse sequence, as depicted in Figure 3a, and monitoring the stimulated echo amplitude $A(t_m;\tau_1)$ at a given pulse delay τ_1 as a function of the mixing time t_m, we probe a single-particle reorientational correlation function.[15,16,18] Explicitly,

$$A(t_m;\tau_1) \propto \langle \sin[\omega(0)\tau_1] \sin[\omega(t_m)\tau_1] \rangle \equiv f(t_m;\tau_1) \qquad (2)$$

Here $\omega(t)$ defines the NMR frequency (in the rotating frame) and is given by $\omega(t) = (\delta/2)(3\cos^2\vartheta(t) - 1)$ with an orientation of the axially symmetric chemical shift tensor of the molecule at an angle $\vartheta(t)$ with respect to the external magnetic field and $\delta = 2\pi(^2/_3\Delta\sigma\nu_0)$. In the limit $\tau_1 \rightarrow 0$ the correlation function eq 2 becomes identical with the correlation function $f_2(t)$ of the second Legendre polynomial P_2[16,18]

$$A(t_m;\tau_1 \rightarrow 0) \propto (\tau_1\delta)^2 \langle P_2[\cos(\vartheta(0))]\, P_2[\cos(\vartheta(t_m))] \rangle \equiv f_2(t_m) \qquad (3)$$

Experimentally, however, the limit $\tau_1 \rightarrow 0$ cannot be reached because the echo amplitude is zero under this condition. Moreover, the finite length of the radio frequency pulses τ_{rf} presents a limit for small τ_1 as $\tau_1 > \tau_{rf}$. For nonzero delay τ_1 the correlation function $f(t_m;\tau_1)$ decays to the plateau value $f_\infty(\tau_1)$ at $t_m \rightarrow \infty$ and can be expressed as[15,18]

$$A(t_m;\tau_1) \propto [(1 - f_\infty(\tau_1))F(t_m;\tau_1) + f_\infty(\tau_1)] \qquad (4)$$

For $t_m \rightarrow \infty$ the normalized function $F(t_m;\tau_1)$ decays to zero and $f_\infty(\tau_1)$ describes the remaining reorientational correlation for a given τ_1. The functions $F(t_m;\tau_1)$ and $f_\infty(\tau_1)$ can be calculated numerically for a given type of motional process.[16,18] In the case of supercooled TPP the experimentally found function $f_\infty(\tau_1)$ is well reproduced by assuming a uniform, i.e., isotropic, distribution of the orientation of the TPP molecules on the surface of a sphere, as expected for a liquid at long times. A comparison between experimentally observed $f_\infty(\tau_1)$ and the theoretical calculation is displayed in Figure 5a. The calculated curve is shifted to the left by 2.5 μs to take into account finite pulse lengths. It was found that at $\tau_1 < 15$ μs the function $F(t_m;\tau_1)$ becomes independent of τ_1, and thus the approximation $F(t_m;\tau_1) \cong F_2(t_m)$ is justified, where $F_2(t_m)$ is the normalized correlation function of the second Legendre polynomial. For the subsequent measurements $\tau_1 = 10$ μs was chosen.

For long times t_m the stimulated echo is damped by spin−lattice relaxation, which, therefore, has to be measured independently to single out the effects of molecular motion. Thus, the actually measured echo amplitude has to be decribed by

$$A(t_m;\tau_1) \propto [(1 - f_\infty(\tau_1))F(t_m;\tau_1) + f_\infty(\tau_1)] \exp(-t/T_1) \qquad (5)$$

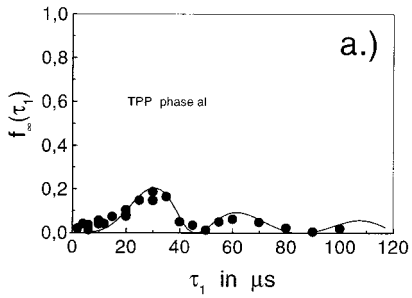

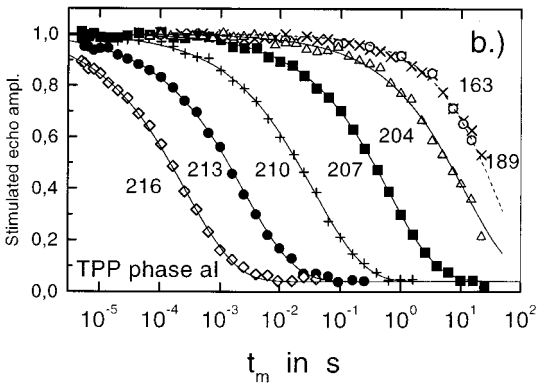

Figure 5. (a) $f_\infty(\tau_1)$ as obtained by fitting the stimulated echo decay with eq 6 in the supercooled liquid (points) and calculated for an isotropic molecular reorientation with applying $\Delta\sigma\nu_o = 38.3$ kHz (solid line). The calculated curve is shifted to the left by 2.5 μs to take into account finite pulse lengths. (b) Stimulated echo decays in supercooled TPP (phase aI). Numbers indicate temperature in K. The delay τ_1 was set to 10 μs. Spin−lattice relaxation is taken into account. At 163 K and 189 K spin diffusion dominates the experimental data; at 204 K also the effect of spin diffusion is taken into account (cf. text). Dashed line: KWW fit at 163 K with the parameters $\tau_{KWW} = 40$ s and $\beta = 0.72$. Solid lines: KWW fits with eq 6 and $\beta = 0.52$.

Figure 5b presents the normalized stimulated echo decays in the supercooled liquid and the glass (as measured with τ_1=10 μs) after correcting for the T_1 effect (cf. eq 5). T_1 for each temperature was measured in an independent experiment (cf. below). Below 190 K no temperature dependence of the stimulated echo decay was observed any longer. This fact indicates that well below the glass transition temperature ($T_g = 205$ K) spin diffusion, mediated via dipolar coupling of the nuclei, dominates the echo decay, whereas for higher temperatures molecular motion leads to a strong temperature dependence of the echo decay curves. The decay curves are nonexponential and are well interpolated by a Kohlrausch−Williams−Watts (KWW) function $\exp(-(t/\tau_{KWW})^\beta)$. This behavior is typical of the main relaxation (α-process) in supercooled viscous liquids.[19−21] The decay dominated by spin diffusion at $T < 190$ K can also be described by a KWW function. Here, the parameters $\beta = 0.72$ and $\tau_{KWW} = 40$ s provide a satisfying interpolation (dashed line in Figure 5b). To take into account the contribution of spin diffusion at $T > 190$ K, we divided the experimentally observed echo decay curves by this low-temperature KWW decay (in addition to correcting for T_1 effects). This led to a slight change of the decay at 204 K, while at higher temperatures spin-diffusion effects can be safely neglected. We note once again that by

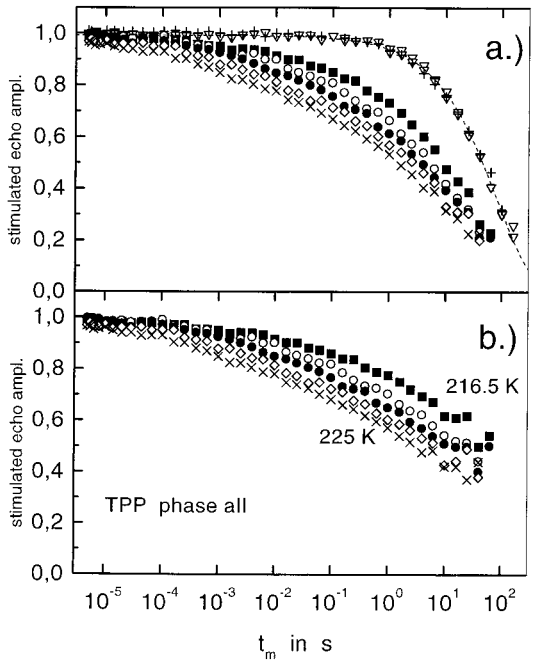

Figure 6. Stimulated echo decays in TPP phase aII at different temperatures: 183 K (▽); 203 K (+); 216.5 K (■); 219 K (○); 221 K (●); 223 K (◇); 225 K (×). The delay τ_1 was set to 10 μs; relative initial intensities are corrected according to the Curie law. (a) Echo decays after taking into account spin−lattice relaxation. At 183 and 203 K spin-diffusion dominates. Dashed line: KWW fit of data at 183 K with $\tau_{KWW} = 79$ s, $\beta = 0.65$. (b) Echo decays after taking into account spin diffusion on the basis of the KWW fit at 183 K.

applying an additional phase cycling (cf. Figure 3a) at least seven decades in time can be probed by applying the stimulated echo technique, which is significantly more than previously reported.[15]

In Figure 5b we included the KWW interpolation of the decay curves. To take into account the small plateau level $f_\infty(\tau_1)$, we fitted the echo decay as

$$A(t_m) \propto [(1 - f_\infty(\tau_1)) \exp(-(t_m/\tau_{KWW})^\beta) + f_\infty(\tau_1)] \quad (6)$$

introducing $f_\infty(\tau_1) = 0.04$ for all temperatures, as obtained from experimental data in Figure 5a. A temperature independent stretching parameter $\beta \cong 0.52$ was found, which is typical of supercooled liquids. The correlation time τ for the KWW function is defined by[22]

$$\tau = \tau_{KWW}\Gamma(1/\beta)/\beta \quad (7)$$

where Γ is the gamma function. The time constant is plotted as a function of temperature in Figure 15 and will be discussed below.

Next we investigated the stimulated echo decay in the newly discovered phase aII. Figure 6a displays the corresponding decay curves after having taken into account the spin−lattice relaxation. Again, the delay τ_1 was set to 10 μs. The relative intensities at different temperatures are corrected according to the Curie law, because the form of the decay curves is not known a priori. No complete decay was observed in the accessible time window of the stimulated echo method. At lowest temperatures again spin diffusion is the dominating factor and no changes with temperature are observed. However, at higher temperatures ($T > 210$ K) the decay is significantly shorter and varies with temperature. Qualitatively, the observed changes of the echo decay can be explained analogously to those

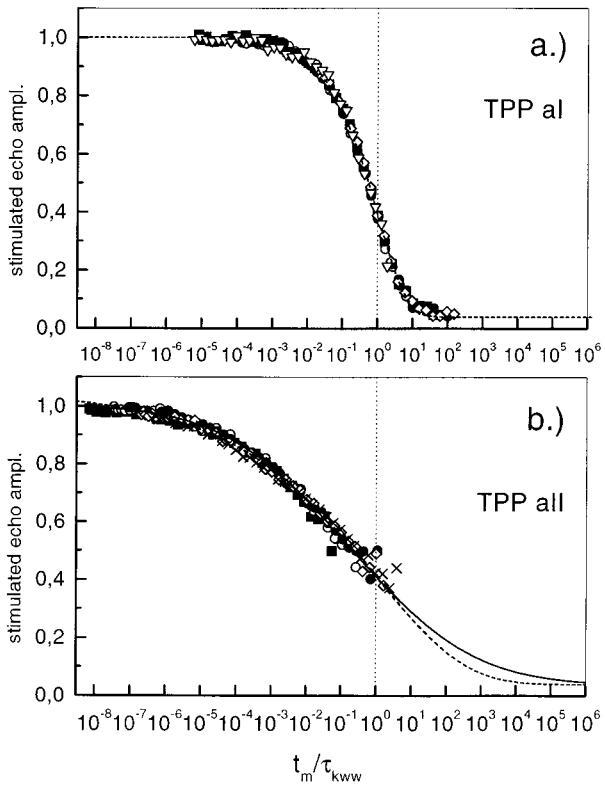

Figure 7. Master curves for the stimulated echo decay in TPP: data are plotted as a function of reduced mixing time t_m/τ_{KWW}, where τ_{KWW} is the time constant of the KWW fit. (a) Supercooled liquid: 204 K (▽); 207 K (■); 210 K (+); 213 K (●); 216 K (◇); (dashed line) KWW fit with $\beta = 0.52$. (b) aII phase: 216.5 K (■); 219 K (○); 221 K (●); 223 K (◇); 225 K (×); (dashed line) KWW fit with $\beta = 0.172$; (solid line) log−Gauss fit with $\sigma = 9.0$ and $\tau = 0.274$ s (cf. eq 8).

found in the supercooled liquid phase: As temperature rises, molecular motion accelerates. Figure 6b shows the echo decays after having corrected the spin-diffusion effects. The latter was taken into account by assuming a KWW decay with $\beta = 0.65$ and $\tau_{KWW} = 79$ s as observed at $T = 183$ K. Although measured at higher temperature, as compared with the supercooled liquid, the correlation loss in phase aII is slower and considerably more nonexponential than the one in the supercooled liquid. As seen in Figure 6b, the correlation loss reaches 60% in the accessible time window.

To get more information on the shape of the correlation function, we assumed that the shape of the decay curves does not change within the small temperature interval investigated and a master curve is constructed by shifting the loss curves of Figure 6b on the logarithmic time scale in an appropriate way. As demonstrated in Figure 7b, indeed a master curve is obtained in fair approximation. For comparison, the corresponding master curve for the supercooled liquid is shown in Figure 7a. When both master curves are compared, it is once again obvious that a significantly different correlation loss occurs in both phases. The correlation loss in phase aII seems to extend at least over twice as many decades in time as compared to that of phase aI. Such extremely stretched orientational correlation functions are usually not observed in neat molecular liquids.

For a quantitative analysis we assume that the motional process in phase aII is qualitatively similar to the motion in the supercooled liquid in the sense that molecular motion leads to complete loss of correlation at sufficiently long times. In other words, we assume, as aforementioned, that the orientations of the molecules redistribute isotropically. This assumption will be further substantiated below, where the results from the 2D

spectra and from dielectric relaxation are discussed. Thus, we again apply a KWW function to interpolate the data (dashed lines in Figure 7b). The plateau level is fixed to $f_\infty(\tau_1) = 0.04$, as found in the supercooled liquid. As expected, the fit yields an extremely small stretching parameter $\beta = 0.17$. The corresponding τ_{KWW} values, calculated from the scaling factors in Figure 7b, are in the range of hundreds of seconds. According to the very low value of the stretching parameter β, the corresponding mean correlation times are on the order of 10^4 s (cf. eq 7).

Previously,[4] we applied a log−Gauss spectral shape to fit the imaginary part of the complex permittivity. Therefore, we also applied the log−Gauss distribution to interpolate time domain data in Figure 7b. The solid line in Figure 7b represents the corresponding fit by superimposing exponential decays with the distribution $G(\ln \tau)$

$$G(\ln \tau) = (\pi\sigma^2)^{-1/2} \exp[-\ln^2(\tau/\tau_0)/\sigma^2] \qquad (8)$$

The fit parameter is $\sigma = 9.0$. The quantity $\ln \tau_0$ can be identified with the mean logarithmic correlation time $\langle \ln \tau \rangle$. The mean correlation time $\langle \tau \rangle$ is given in good approximation by[23,24]

$$\tau \equiv \langle \tau \rangle = \tau_0 \exp(\sigma^2/4) \qquad (9)$$

and is in the range of 10^9-10^{11} s. Both fitting functions nearly coincide in the experimentally observed time range and well fit the experimental points. However, they differ at longer times where no experimental points can be compiled. Note that the average correlation time $\langle \tau \rangle$ is strongly determined by the long time behavior whereas this is not the case for $\langle \ln \tau \rangle$. Correspondingly, for such an extremely stretched function and a very broad distribution of correlation times, the differences between the averages $\ln\langle \tau \rangle$ and $\langle \ln \tau \rangle$ may become extremely large. A similar behavior is found for secondary processes in glasses.[23,24] Also, the difference of both fitting functions, namely the KWW and the Gaussian convolution decay, leads to different estimates for the mean correlation times $\langle \tau \rangle$. In any case, the obtained $\langle \tau \rangle$ are not well defined because the long-time end of the correlation function is not resolved by the NMR experiment. Therefore, only $\langle \ln \tau \rangle$, obtained from the Gaussian fit, is collected in Figure 15 and discussed below.

3. 2D spectra. In the 2D NMR exchange spectrum $S(\omega_1,\omega_2;t_m)$ the orientation-dependent frequencies $\omega_1(\vartheta(t_1))$ and $\omega_2(\vartheta(t_2))$ before and after the mixing time t_m (see Figure 3b) are correlated so that $S(\omega_1,\omega_2;t_m)$ describes the joint probability density of finding the molecule with the frequency ω_1 in the evolution period t_1 and the frequency ω_2 in the detection period t_2. The joint probabilities for various motional processes and the correspondent 2D spectra have been calculated, e.g., in ref 16.

To get the 2D pattern characterized by complete exchange, the condition $t_m \gg \tau$ must hold. On the other hand, because of a reduced signal-to-noise ratio at a mixing time comparable with the spin−lattice relaxation time T_1, also the condition $t_m \leq T_1$ has to be satisfied. Both conditions are easily fulfilled in the case of the supercooled liquid TPP at temperatures higher than 206 K, and the corresponding experimental 2D spectrum measured at 210 K is shown in Figure 8 (a, left) for a mixing time $t_m = 2$ s. In phase aII, however, the correlation function is extremely stretched. Because of that, the full exchange conditions cannot be achieved experimentally in phase aII, and consequently only a partial exchange pattern was observed. This is shown in Figure 8 (b, left) for a temperature $T = 223$ K and a mixing time $t_m = 10$ s. We note that the stability of the phase during measuring the 2D spectrum with respect to crystallization was controlled by measuring the spin−lattice time before and after the experiment.

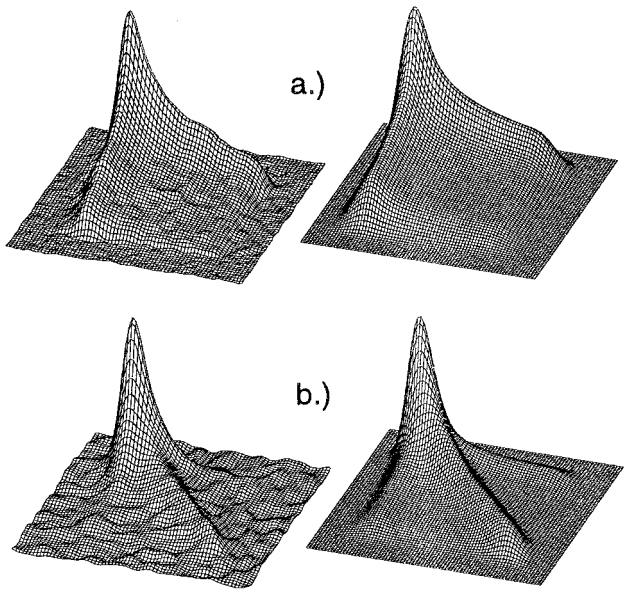

Figure 8. Experimental (left-hand) and numerically simulated (right-hand) ^{31}P 2D exchange spectra of TPP: (a) supercooled liquid (phase aI) at 210 K and mixing time $t_m = 2$ s and (b) second amorphous phase (aII) at 223 K and mixing time $t_m = 10$ s. The spectra are symmetrized and a Gaussian broadening of 4 kHz was used; Δ_1 and Δ_2 were set to 20 μs.

The 2D spectrum of phase aI acquired using a mixing time $t_m = 2$ s $\gg \tau$ is well represented by a uniform redistribution of the molecular orientation. The corresponding calculated 2D spectrum is included in Figure 8 (a, right). Upon inspection of the 2D spectrum in phase aII, it is well recognized that no traces of ellipsoid off-diagonal pattern were observed, which appear if discrete large angle jumps are involved.[16] But rather the off-diagonal intensity is distributed over the entire $\omega_1-\omega_2$ plane, as is the case in the 2D spectrum of phase aI. This is even more clearly seen when the contour plots of the 2D spectra are considered (cf. Figure 9). We take this as an indication that essentially uniform redistribution is involved also in phase IIa. Because no complete exchange was observed in the 2D spectrum, we have to specify the way the molecules achieve the uniform redistribution in order to simulate the 2D spectrum. Thus, we further assume that the reorientation proceeds via rotational diffusion. For a simulation of a partially exchanged 2D spectrum, it is sufficient to determine the reorientation-angle distribution function $R(\beta;t_m)$ for a given motional model. This function specifies the distribution of the chemical shift tensor orientation β after a mixing time t_m relative to its direction at the beginning of the mixing time t_m. The 2D spectrum $S(\omega_1,\omega_2;t_m)$ can then be expressed (assuming a symmetric chemical shift tensor) by

$$S(\omega_1,\omega_2;t_m) = \int_0^{90} R(\beta;t_m)\, S_\beta(\omega_1,\omega_2)\, d\beta \qquad (10)$$

where $S_\beta(\omega_1,\omega_2)$ is the 2D subspectrum corresponding to a given β and is independent of the assumed motional process. The function $R(\beta;t_m)$ was calculated by the numerical solution of the rotational diffusion equation with a single correlation time τ. For details see the Appendix.

By inspection of the calculated 2D spectra it became obvious that the experimental spectrum, which contains both an intensive

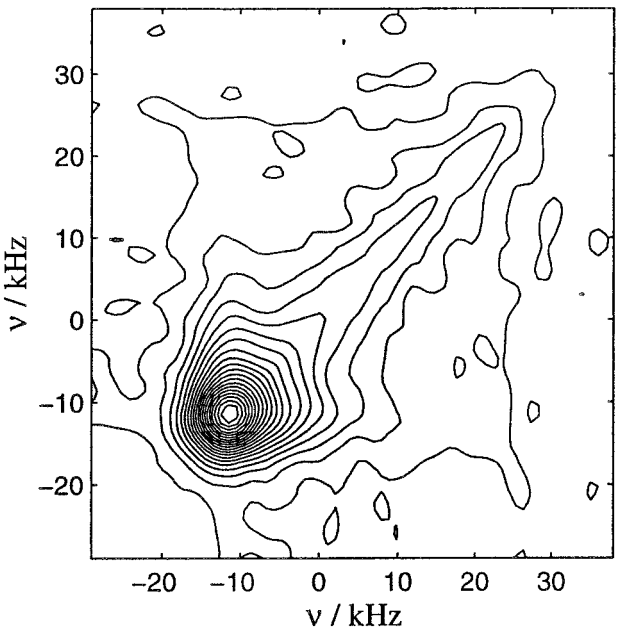

Figure 9. Contour plot of the measured 2D spectrum of TPP phase aII displayed in Figure 8. Clearly, the exchange intensity is spread over the whole spectral plane.

diagonal and wings along ω_1 and ω_2 directions, cannot be described by the model with a single correlation time. Instead, a superposition of many 2D patterns with different τ has to be taken. Therefore, we applied again a distribution of correlation times $G(\ln \tau)$. In particular, we took $G(\ln \tau)$ from the one applied for the simulation of the stimulated echo decay. 2D spectra were calculated for a number of correlation times equally distributed on logarithmic scale. The complete 2D spectrum taken as a superposition of these subspectra with the corresponding weight is shown in Figure 8b (right). The calculated 2D spectrum reproduces all features of the measured one. In particular, the intensive diagonal and wings in ω_1 and ω_2 directions are well reproduced. We note that a similar approach was chosen in order to describe the 2D spectra of polystyrene or polyisoprene above T_g.[16] Finally, we mention that at a mixing time $t_m = 10$ s the spin-diffusion accounts for about 15% correlation loss (cf. Figure 6); however, this cannot explain the observed 2D exchange pattern.

Summarizing this part, we have presented a consistent description of the 2D experiments (in both time and frequency domain) carried out for the two phases of TPP by suggesting uniform orientational redistribution in both phases.

4. Spin−Lattice Relaxation. In our previous publication[4] some preliminary measurements of the spin−lattice relaxation times T_1 in the supercooled liquid, in phase aII, and in the crystalline phase of TPP were reported. The relaxation is monoexponential in both phases aI and aII. In Figure 10a we summarize the relaxation data obtained, covering now a broader temperature range as compared to that reported in ref 4. T_1 in phase aII is somewhat longer with repect to that in the supercooled liquid, but considerably shorter than T_1 in the crystal. In comparison with the crystal, both phases aI and aII exhibit a strong temperature dependence of T_1, indicating the presence of molecular motion. The observed T_1 minimum in phase aI is typical of viscous liquids. To estimate the correlation time τ at the minimum, we apply the relationship $\omega_0\tau \cong 1$, which leads to $\tau \cong 9.9 \times 10^{-10}$ s at $T = 266$ K (cf. Figure 15). At low temperatures the temperature dependence of T_1 in the supercooled liquid becomes flatter, again a typical behavior

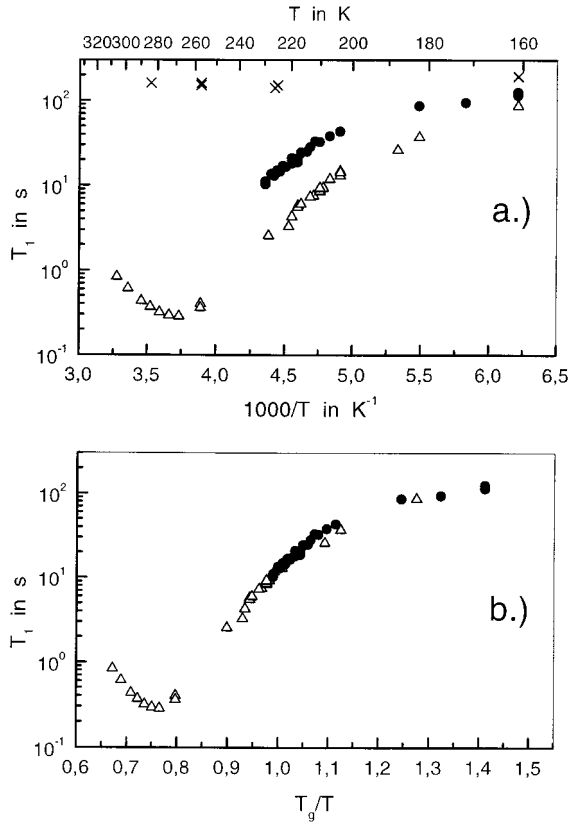

Figure 10. ^{31}P spin−lattice relaxation times in the different phases of TPP: (△) phase aI, (●) phase aII, (×) crystal; (a) as a function of reciprocal temperature; (b) as a function of reduced reciprocal temperature T_g/T. T_g(aI) = 205 K, T_g(aII) = 227 K.

observed in the supercooled liquid entering the glassy state (T_g = 205 K). Qualitatively, a similar $T_1 = T_1(T)$ dependence is observed in phase aII. To further demonstrate this similarity of the respective temperature dependence, we plotted T_1 as a function of the reduced reciprocal temperature T_g/T in Figure 10b. For phase aII we tentatively chose $T_g^{aII} = 227$ K. As reported,[3,4] peculiarities in the DSC trace in the temperature range 210 K < T < 225 K are observed, which might be interpreted as a broad step in the heat capacity, indicating a glass transition in phase aII. A high similarity of the $T_1(T_g/T)$ curves results and may indicate that phase aII behaves in this respect similar to the supercooled liquid. More precisely, in the slow motion limit ($\omega_0\tau \gg 1$) the temperature dependence of T_1 is given by $T_1 \propto \tau^b$,[15] where the exponent b specifies the frequency dependence of the spectral density. In the case of a Cole−Davidson spectral density[25] $b = \beta_{CD}$ holds (cf. below). Thus, a similar temperature dependence of T_1 signifies that b [(d log τ)/(d1/T)] is similar (assuming b to be temperature independent). Since b is somehow similar in both systems (cf. Figure 11 and section 5), essentially the same temperature dependence of the correlation time is found. This is confirmed by comparing the time constants obtained from the stimulated echo analysis in both phases (cf. Figure 15).

5. Dielectric Spectroscopy. In our previous publication we also reported on dielectric measurements of both amorphous phases of TPP.[4] Whereas, in the supercooled liquid, spectra typical of the α-relaxation were found, a broad more or less symmetric relaxation peak was observed in phase aII. Upon heating, this broad maximum is shifted to higher frequencies. This is demonstrated in Figure 11 where the imaginary part $\epsilon''(\nu)$ of the complex susceptibility is plotted. In the present study

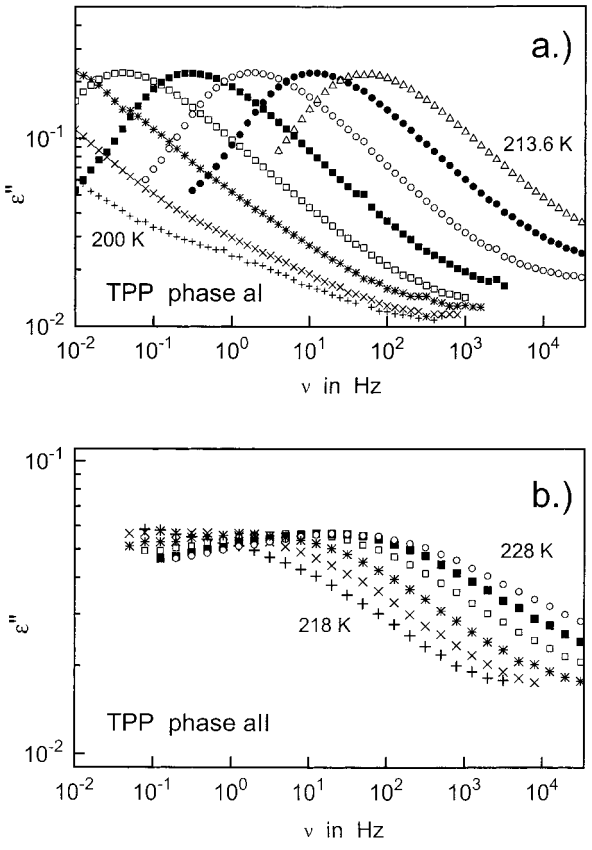

Figure 11. Dielectric susceptibility $\epsilon''(\nu)$ of TPP as a function of frequency ν. (a) Phase aI: (+) 200 K; (×) 202 K; (∗) 203.7 K; (□) 205.7 K; (■) 207.7 K; (○) 209.6 K; (●) 211.7 K; (△) 213.6 K. (b) Phase aII: (+) 218 K; (×) 220 K; (∗) 222 K; (□) 224 K; (■) 226 K; (○) 228 K.

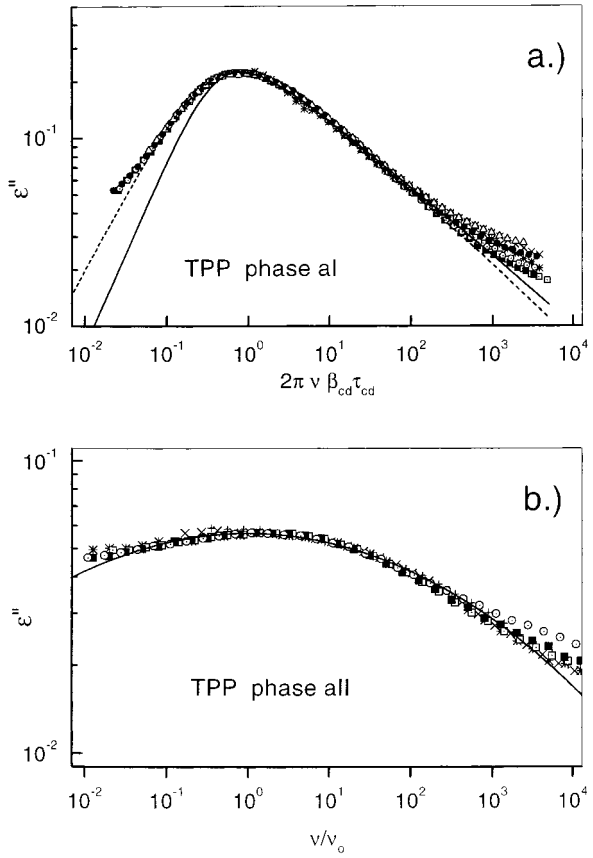

Figure 12. Master curve of dielectric susceptibility $\epsilon''(\nu)$ of TPP. (a) $\epsilon''(\nu)$ of the supercooled liquid rescaled with $2\pi\nu\beta_{CD}\tau_{CD}$, where β_{CD} and τ_{CD} are the parameters of Cole−Davidson fit: (×) 202 K; (∗) 203.7 K; (⊡) 205.7 K; (■) 207.7 K; (⊙) 209.6 K; (●) 211.7 K; (△) 213.6 K; (solid line) CD fit with $\beta_{CD} = 0.36$, $\tau_{CD} = 0.44$ s, $\Delta\epsilon = 0.77$; (dashed line) HN fit with $\alpha_{HN} = 0.17$, $\beta_{HN} = 0.47$, $\tau_{HN} = 0.45$ s, and $\Delta\epsilon = 0.83$. (b) $\epsilon''(\nu)$ of phase aII as function of resacled frequency ν/ν_0, where ν_0 is the central frequency of the log−Gauss fit: (+) 218 K; (×) 220 K; (∗) 222 K; (⊡) 224 K; (■) 226 K; (⊙) 228 K; (solid line) log−Gauss fit with $\sigma = 8.6$, $\nu_0 = 1$ Hz, and $\Delta\epsilon = 0.55$.

dielectric measurements were performed in an extended temperature range, and we want to address the question whether the dielectric permittivity and the NMR stimulated echo data may be consistently interpreted.

Figure 12 shows the "master" curve for the imaginary part of the dielectric losses $\epsilon''(\nu)$ that was obtained by shifting each curve with respect to the logarithmic frequency scale. The loss curve in phase aII is significantly broader as compared to that of phase aI, and the loss at the maximum in phase aII is by a factor of 4 smaller than that in phase aI. This highly resembles the NMR findings: The apparent distribution of correlation times is extremely broad in phase aII. To obtain the time constant, the spectral shape in the supercooled liquid was interpolated by a Cole−Davidson (CD) function[25]

$$f_{CD}(\nu) = \Delta\epsilon\ \mathrm{Im}[(1 + \mathrm{i}2\pi\nu\tau_{CD})^{-\beta CD}] \qquad (11)$$

with the parameters $\beta_{CD} = 0.36$, $\tau_{CD} = 0.44$ s, and $\Delta\epsilon = 0.77$ (phase aI), where $\Delta\epsilon$ is the relaxation strength (cf. solid line in Figure 12a). Data of Figure 12a are shown in reduced frequency scale $\omega_0\tau = 2\pi\nu_0\beta_{CD}\tau_{CD}$. Note that the CD function provides a poor interpolation at low frequencies. Nevertheless, a reasonable estimate of the correlation time $\tau = \tau_{CD}\beta_{CD}$ is obtained and plotted in Figure 15. The thus obtained time constants agree very well with those recently reported by Schiener et al.[26] The dashed line in Figure 12a is an interpolation by the Havriliak−Negami (HN) function[25]

$$f_{HN}(\nu) = \Delta\epsilon\ \mathrm{Im}[(1 + (\mathrm{i}2\pi\nu\tau_{HN})^{-\alpha_{HN}})^{\beta_{HN}}] \qquad (12)$$

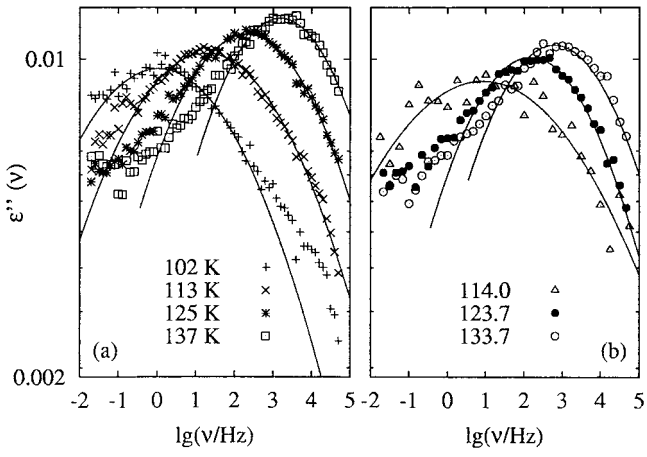

Figure 13. Dielectric susceptibility $\epsilon''(\nu)$ of TPP as a function of frequency ν at low temperatures (β-process). (a) Phase aI: (+) 102 K; (×) 113 K; (∗) 125 K; (⊡) 137 K. (b) Phase aII: (△) 114 K; (●) 123.7 K; (⊙) 133.7 K.

with the parameters values $\alpha_{HN} = 0.17$, $\beta_{HN} = 0.47$, $\tau_{HN} = 0.45$ s, and $\Delta\epsilon = 0.83$ (phase aI). The HN function provides a satisfying fit.

To describe $\epsilon''(\nu)$ in phase aII, we assumed a log−Gaussian spectral shape

$$f_{LG}(\nu) = \Delta\epsilon(\pi W^2)^{-1/2} \exp[-(\ln^2(\nu/\nu_0)/W^2] \qquad (13)$$

as shown in Figure 12b, solid line. There the data are plotted as a function of the rescaled frequency (ν/ν_0). Equation 13 may be considered as a convolution of a Debye susceptibility with a very broad Gaussian distribution of correlation times $G(\ln \tau)$.[26] Within this approach the average logarithmic correlation time is defined by $\langle \log \tau \rangle = -\log(2\pi\nu_0)$ and displayed in Figure 15. The distribution width $W = 8.6$ is in good agreement with that obtained from the NMR stimulated echo decay $\sigma = 9.0$, and a relaxation strength $\Delta\epsilon = 0.55$ is found.

It is interesting to compare the relaxation strength $\Delta\epsilon$ in both amorphous phases of TPP. Applying the HN fit for the data of the supercooled liquid and the Gaussian fit for the data in phase aII we find $\Delta\epsilon^{(aII)} \approx 0.66\Delta\epsilon^{(aI)}$. Of course, this can only be a rough estimate because we are not able to measure the dielectric loss at low frequencies in the case of phase aII, and thus any estimate of $\Delta\epsilon$ depends on the model function chosen. For example, also for phase aII the HN function provides a somewhat better interpolation, yielding a relation $\Delta\epsilon^{(aII)} \approx 0.76\Delta\epsilon^{(aI)}$. Also, we neglected the temperature dependence of $\Delta\epsilon$, but this is a minor effect because the temperature interval studied is small. We conclude that the relaxation strength is similar in both phases.

Cooling the supercooled phase aI significantly below T_g reveals a secondary relaxation ($T \leq 140$ K). This is demonstrated in Figure 13a. A similar relaxation process is also observed for phase aII at these temperatures (Figure 13b). Again it is possible to interpolate the loss by applying a Gaussian susceptibility function of eq 13. The corresponding logarithmic time constant $\langle \log \tau \rangle$ is included in Figure 15. Clearly, these time constants follow an Arrhenius temperature dependence, and they are essentially the same in both phases. We find a mean activation energy $\langle E \rangle = 22.3$ kJ/mol and an exponential prefactor 4.3×10^{-13} s. Upon inspection of the width parameter $W(T)$ of the susceptibility function, it increases with $1/T$, as demonstrated in Figure 14. This is well understood in terms of a distribution of activation energies. Thus the secondary relaxation exhibits features of the Johari β-process as found in many simple glass formers.[23,27] However, we note that the activation energy $\langle E \rangle$ observed here does not obey the recently found behavior $\langle E \rangle \approx 24RT_g$,[27] but rather $\langle E \rangle = 13RT_g$ is observed.

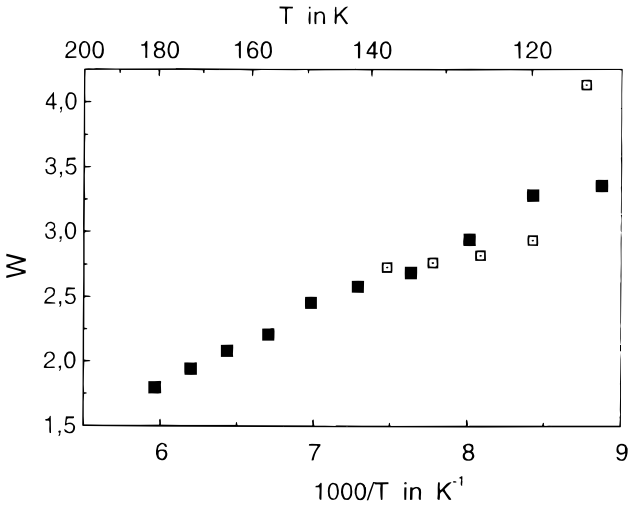

Figure 14. Temperature dependence of the width parameter W of the susceptibility function for the β-process: (■) phase aI; (⊡) phase aII.

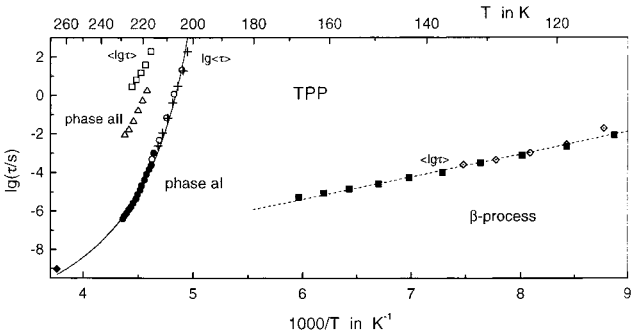

Figure 15. Mean correlation times $\log \langle \tau \rangle$ and mean logarithmic correlation times $\langle \log \tau \rangle$ for main and secondary relaxation as estimated from the analysis of NMR and dielectric data. Main relaxation, phase aI: (+) dielectric spectroscopy; (○) NMR stimulated echo; (◆) T_1 minimum; (●) from ref 26; (solid line) fit by a Vogel−Fulcher−Tammann law, i.e., $\tau = A \exp(B/(T - T_0))$ with $A = 6.2 \times 10^{-14}$ s, $B = 753$ K, $T_0 = 182$ K. Phase aII: (□) NMR stimulated echo; (△) dielectric spectroscopy. Secondary relaxation process: mean logarithmic correlation times from dielectric spectroscopy: (■) phase aI; (◇) phase aII.

Discussion

We applied several methods in order to characterize the molecular motion in the newly discovered, apparently amorphous phase aII of TPP. For comparison, also the conventional supercooled liquid was studied. All experiments carried out clearly demonstrate the presence of motion in phase aII, the time scale of which was estimated in each experiment. However, revealing the geometry of motion is a much more ambitious task. Usually, the most promising method to resolve slow reorientational processes is 2D NMR. This has been once again demonstrated in the case of the supercooled phase (aI) of TPP. We clearly have proven that the molecular reorientation leads to an isotropic redistribution, as expected for a liquid, and the correlation times achieved from NMR and dielectric spectroscopy agree well (cf. Figure 15). However, in the case of phase aII also NMR comes to its limits because the loss of correlation extends over an extremely large frequency and time interval, respectively. Obviously, more than seven decades in time are needed in order to probe the complete loss. Moreover, very long correlation times on the order of 100 s are involved (cf. Figure 6). These extremely stretched decay curves correspond to a very broad dielectric loss (cf. Figure 11). In fact, the low-frequency part of the loss also cannot be resolved by dielectric spectroscopy. Therefore, the long-time behavior of the molecular reorientational correlation function remains an open question. Accordingly, the estimate of the mean logarithmic time constant $\langle \log \tau \rangle$ compiled in Figure 15 is somehow ambiguous although similar temperature dependences are reported from both NMR and dielectric spectroscopy. The difference found in the absolute values of $\langle \log \tau \rangle$ for the two methods indicates that the log−Gaussian distribution does not fully describe the data. Probably, the long time tail of $G(\ln \tau)$ is underestimated (cf. Figure 11). As previously reported, the temperature dependence of $\langle \log \tau \rangle$ is described by an apparent activation energy of 250 kJ/mol. However, a small tendency for a non-Arrhenius behavior can be recognized. Moreover, the unphysically small exponential prefactor suggests that a non-Arrhenius behavior is also expected for phase aII.

Concerning the geometry of the reorientational process in phase aII, we have assumed isotropic rotational diffusion as in the case of the supercooled liquid aI. Five indications favor this interpretation: (i) In the 2D spectrum of phase aII no discrete off-diagonal intensities are found, but rather a continuous redistribution over the plain is observed. That is, the reorientational process explores essentially all angles in the course of

time, leading to a isotropic orientational redistribution for sufficiently long times. A simulation within the model of rotational diffusion describes the 2D spectrum well. (ii) The strength of the dielectric loss appears to be quite similar in both phases. Thus, assuming that the Kirkwood factor is not different in both phases, molecular motion relaxes the same amount of polarization. As a consequence, the motional geometry is expected to be similar. Of course, this comparison of the relaxation strength also relies on a proper estimate of the shape of the loss curve. (iii) As already mentioned, the high value of activation energy and the nonphysical inverse attempt frequency of the Arrhenius law indicate that no single particle motion is involved. Both quantities are similar to those in the supercooled liquid (cf. Figure 15). (iv) In both phases a secondary process is found that exhibits very similar features and can be interpreted as a Johari−Goldstein β-process. In the crystal state this process is not found, at least not at comparable temperatures. (v) The spin−lattice relaxation times in both phases aI and aII are very similar in the sense that their temperature dependence can be scaled by introducing a glass transition temperature $T_g = 227$ K for phase aII that is 22 K higher than the one for phase aI. Assuming that the spectral density exponents b (at $\omega_o\tau > 1$) (cf. Spin−Lattice Relaxation section, above) are similar (cf. Figure 11), it follows that the temperature dependences of the correlation times are similar in both phases. We think in particular that points i and ii suggest essentially uniform orientational redistribution in phase aII.

This reorientational behavior may be found, as mentioned, in liquids but also in supercooled plastically crystalline phases. Because we do not find Bragg reflexes, we exclude the possibility of a crystalline phase. In any case the phase transformation from aI to aII is not quenching molecular motion. However, the correlation function in phase aII exhibits features that have not been reported for neat molecular systems. The extent of nonexponential decay is extreme. Even in polymers the correlation functions are usually less stretched. Hédoux et al.[6] claimed the existence of "nanocrystallized domains" because "the local order in the glacial state is a very clear picture of the crystalline symmetry." However, we think the reorientational correlation function is atypical of a crystal environment.

The possibility that phase aII is a liquid crystal was raised by Johari and Ferrari.[5] Because the long-time behavior of the reorientational correlation function, as studied by NMR, for example, cannot be probed experimentally, we cannot completely exclude this interpretation. Upon inspection of Figure 7, the correlation function is found to decay down to 0.35, at least. Assuming a nematic liquid crystal the long-time limit of the correlation function $F_2(t)$ is given by S^2 where S is the order parameter.[28] Therefore, the upper limit estimate of the order parameter is $S \cong 0.6$. However, several findings can be compiled that do not favor the hypothesis of phase aII being a liquid crystal: (i) The correlation function is too broad as compared to that usually found in low molecular weight nematic liquid crystals. (ii) Usually, the enthalpy change from a liquid to a nematic liquid crystal is small. However, in the case of TPP a strong change was observed. (iii) According to prelimary molecular modeling, the structure of the molecule is essentially described by a globular shape. Due to geometric hindering, the phenyl rings are in twisted position to each other. Therefore, no high molecular anisotropy and thus no tendency for orientational ordering is expected. We emphasize that the DSC behavior found for TPP is also different from the behavior of a monotropic nematic liquid crystal where the liquid crystal is only observed upon cooling the liquid. In any case the dynamics in phase aII is extremely slow and a macroscopic ordering is not expected. Therefore, many techniques to probe liquid crystal properties cannot be applied. Finally, we note that phase aII is optically isotropic.[4]

Concluding, we think it is fair to assume that the second amorphous phase of TPP is a highly viscous liquid and the transition from phase aI to aII is a liquid−liquid transition. For example, such a liquid−liquid transition is discussed for supercooled water within an extended van der Waals model, which additionally takes into account hydrogen bondings.[10,11] However, up to our knowledge no such transition has been observed experimentally at ambient pressure. Therefore, the case of TPP deserves further investigation in order to substantiate our conclusion in more detail. In particular, the structural difference in the two liquid phases has to be clarified. A candidate for a special interaction to rationalize two distinguished liquid states for a simple molecule like TPP has still to be searched.

Acknowledgment. The authors appreciate the financial support of the Deutsche Forschungsgemeinschaft through SFB 279 and grant no. Ro 907/3-1.

Appendix

To describe the reorientational process in both phases of TPP, we assumed the presence of rotational diffusion; in other words, the conditional probability to find a certain orientation of a molecule obeys the rotational diffusion equation, which is solved in a discrete form with N angular steps spaced by an increment $\Delta\beta = \pi/N$[29] leading to $\beta_i = (i - {}^1/_2)\Delta\beta$ (here, we took $N = 180$). The resulting discrete master equation reads

$$dP_i/dt_m = \Sigma_k \Pi_{ik} P_k \tag{A1}$$

where $P_i(t_m)$: $= R(\beta_i, t_m)$ ($i = 1, ..., N$), and Π is a tridiagonal exchange matrix with the nonzero elements[16]

$$\Pi_{m,m+1} = 1/(6\tau\Delta\beta^2)\,\sin(m\Delta\beta)/\sin[(m + {}^1/_2)\Delta\beta] \tag{A2a}$$

$$\Pi_{m+1,m} = 1/(6\tau\Delta\beta^2)\,\sin(m\Delta\beta)/\sin[(m - {}^1/_2)\Delta\beta] \tag{A2b}$$

$$\Pi_{m,m} = -2/(6\tau\Delta\beta^2)\,\cos(\Delta\beta/2) \tag{A2c}$$

The correlation time is connected to the rotational diffusion constant D_{rot} by $\tau = 1/6D_{rot}$. The exchange matrix eq A2 is diagonalized.

The subspectra $S_\beta(\omega_1,\omega_2)$ are given by[16]

$$S_\beta(\omega_1,\omega_2) = \frac{p_0}{\sqrt{6\delta\left(\omega_1 + \frac{\delta}{2}\right)}\sqrt{6\delta\left(\omega_2 + \frac{\delta}{2}\right)}} \times \frac{1}{\sqrt{\sin^2\beta\left(1 - \frac{2}{3}\left(\frac{\omega_1}{\delta} + \frac{1}{2}\right)\right) - \left\{\pm\frac{2}{3}\left(\frac{\omega_2}{\delta} + \frac{1}{2}\right) \pm \cos\beta\sqrt{\frac{2}{3}\left(\frac{\omega_1}{\delta} + \frac{1}{2}\right)}\right\}^2}} \tag{A3}$$

We calculated the function $R(\beta,t_m)$ and the corresponding 2D exchange spectra according to eq 10 at different ratios t_m/τ.

References and Notes

(1) Ha, A.; Cohen, I.; Zhao, X.; Lee, M.; Kivelson, D. *J. Phys. Chem.* **1996**, *100*, 1.

(2) Cohen, I.; Ha, A.; Zhao, X.; Lee, M.; Fischer, T.; Strouse, M. J.; Kivelson, D. *J. Phys. Chem.* **1996**, *100*, 8518.

(3) Miltenburg, K. van; Blok, K. *J. Phys. Chem.* **1996**, *100*, 16457.
(4) Wiedersich, J.; Kudlik, A.; Gottwald, J.; Benini, G.; Roggatz, I.; Rössler, E. *J. Phys. Chem.* **1997**, *101*, 5800.
(5) Johari, G. P.; Ferrari, C. *J. Phys. Chem. B* **1997**, *101*, 10191.
(6) Hédoux, A.; Guinet, Y.; Descamps, M. *Phys. Rev. B* **1998**, *58*, 31.
(7) Benini, G.; Semmelhack, H. C.; Esquinazi, P.; Rössler, E. Unpublished X-ray scattering results.
(8) Smith, K. H.; Shero, E.; Chizmeshya, A.; Wolf, G. H. *J. Chem. Phys.* **1995**, *102*, 6851.
(9) Mishima, O. *J. Chem. Phys.* **1994**, *100*, 5910.
(10) Angell, C. A.; Shao, J.; Grabow, M. In *Non equlibrium phenomena in supercooled fluids, glasses and amorphous materials*; Giordano, M., Leporini, D., Tosi, M. P., Eds.; World Scientific: Singapore, 1996; p 50.
(11) Poole, P. H.; Sciortino, F.; Grande, T.; Stanley, H. E.; Angell, C. A. *Phys. Rev. Lett.* **1994**, *73*, 1632.
(12) Avrami, M. *J. Chem. Phys.* **1941**, *9*, 177.
(13) Schaefer, D.; Leisen, J.; Spiess, H. W. *J. Magn. Reson.* **1995**, *A115*, 60.
(14) A homonuclear dipolar coupling would result in an appearance of zero and multiple quantum coherences after the second rf pulse, which can be converted in the observable single quantum coherence by the third pulse and, hence, contribute to the measured signal. The intensity of this contribution is proportional to $\langle \sin(\omega_m \tau_1) \rangle$, where ω_m is the strength of homonuclear dipolar interaction estimated to be $\omega_m \approx 2\pi \times 1$ kHz. This term can be neglected for sufficiently short delay $\tau_1 \ll {}^1/_4(1/\omega_m) \approx 40$ μs.
(15) Rössler, E.; Eiermann, P. *J. Chem. Phys.* **1994**, *100*, 5237.
(16) Schmidt-Rohr, K.; Spiess, H. W. *Multidimensional Solid-State NMR and Polymers;* Academic Press: London, 1994.
(17) Previously we reported $\Delta\sigma = 238$ ppm,[4] which is within the experimental error.
(18) Fujara, F.; Wefing, S.; Spiess, H. W. *J. Chem. Phys.* **1986**, *84*, 4579.
(19) Diehl, R. M.; Fujara, F.; Sillescu, H. *Europhys. Lett.* **1990**, *13*, 257.
(20) Rössler, E.; Sillescu, H. *Chem. Phys. Lett.* **1984**, *112*, 94.
(21) Ediger, M. C.; Angell, C. A.; Nagel, S. R. *J. Phys. Chem.* **1996**, *100*, 31.
(22) Lindsey C. P.; Patterson, G. D. *J. Chem. Phys.* **1980**, *73*, 3348.
(23) Kudlik, A.; Rössler, E. *J. Non-Cryst. Solids* **1998**, *235*−*237*, 406.
(24) Richert, R.; Bässler, H. *J. Phys.: Condens. Matter* **1990**, *2*, 2273.
(25) Böttcher, C. J. F.; Bordewijk, P. *Theory of electric polarization*; Elsevier: Amsterdam, 1978; Vol. II.
(26) Schiener, B.; Loidl, A.; Chamberlin, R. V.; Boehmer, R. *J. Mol. Liq.* **1996**, *69*, 243.
(27) Kudlik, A.; Tschirwitz, C.; Benkhof, S.; Blochowicz, T.; Rössler, E. *Europhys. Lett.* **1997**, *40*, 649.
(28) Szabo, A. J. *J. Am. Chem. Soc.* **1982**, *104*, 4546.
(29) Wefing, S.; Kaufmann, S.; Spiess, H. W. *J. Chem. Phys.* **1988**, *89*, 1219.